Three Wide Separation L-Dwarf Companions From the Two Micron All Sky Survey: GL 337C, GL 618.1B, and HD 89744B

AJ, accepted 03 Jul 2001
Preprint typeset using LaTeX style emulateapj v. 14/09/00

THREE WIDE SEPARATION L-DWARF COMPANIONS FROM THE TWO MICRON ALL SKY SURVEY: GL 337C, GL 618.1B, AND HD 89744B[1]

J.C. Wilson[2], J. Davy Kirkpatrick[3], J.E. Gizis[4], M.F. Skrutskie[5], D.G. Monet[6] and J.R. Houck[7]

AJ, accepted 03 Jul 2001

ABSTRACT

We present two confirmed wide separation L-dwarf common proper motion companions to nearby stars and one candidate identified from the Two Micron All Sky Survey. Spectral types from optical spectroscopy are L0 V, L2.5 V, and L8 V. Near-infrared low resolution spectra of the companions are provided as well as a grid of known objects spanning M6 V – T dwarfs to support spectral type assignment for these and future L-dwarfs in the *z'JHK* bands. Using published measurements, we estimate ages of the companions from physical properties of the primaries. These crude ages allow us to estimate companion masses using theoretical low-mass star and brown dwarf evolutionary models. The new L-dwarfs in this paper bring the number of known wide-binary ($\Delta \geq 100$ AU) L-dwarf companions of nearby stars to nine. One of the L-dwarfs is a wide separation companion to the F7 IV-V + extrasolar planet system HD89744Ab.

Subject headings: binaries: general — infrared: stars — stars: low-mass, brown dwarfs

1. INTRODUCTION

The study of binary and multiple systems in the local neighborhood is important for several reasons. It is desirable to have an accurate accounting of stellar systems in the local neighborhood. Improving the statistics of binary primary masses, system mass fractions, orbital separations, and eccentricities are crucial for refining stellar and planetary formation theories. Also, studying wide separation systems in particular gives insight into their dynamic stability with time as a function of orbital separation and mass fraction (and hence binding energy) against disruptive events such as close approaches to giant molecular clouds, stars, and the gravitational potential of the inner Galaxy.

In this paper we present three wide separation L-dwarf companions to nearby stars. One companion has an apparent separation (Δ) of 100 AU $< \Delta <$ 1000 AU, and two have $\Delta >$ 1000 AU. These discoveries, along with similar companions previously reported, highlight the success in searching new portions of binary system phase space (i.e. wide separations) by surveys such as Two Micron All Sky Survey (2MASS; Skrutskie et al. (1997)), the Deep Near-Infrared Survey (DENIS; Epchtein (1997)), and the Sloan Digital Sky Survey (SDSS; York et al. (2000)). The surveys' sensitivities and large areal coverages allow for very low-mass (VLM) stars and brown dwarf companions to be found at separations $\Delta > 100$ AU.[8] The new detections will in turn improve the statistics of systems with mass ratios (q) far from unity.[9] For instance, the low-mass companions already discovered show that the 'brown dwarf desert' at close separation (< 1 % of FGKM main sequence primaries have brown dwarf companions at $\Delta < 3$ AU; Marcy & Butler (2000)) may not extend to wide separations (Gizis et al. 2001a). The added statistics can also be used to test the mass ratio distribution results of Duquennoy & Mayor (1991): their distribution peaks at $q \sim 0.3$ and is then either flat or decreases for $q < 0.2$. Duquennoy & Mayor (1991), however, used the radial velocity technique for searching for unknown companions, a technique poorly suited for discovering $q < 0.1$ systems at wide separation.

The study of VLM stars and brown dwarfs as singular objects also benefits from the discovery of these objects as companions in binary systems. Because brown dwarfs continually cool with time since they cannot sustain hydrogen fusion, and VLM stars near the main sequence limit can take a Hubble time to come to equilibrium, degeneracies occur in the HR diagram for these objects. For example,

[1] Portions of the data presented here were obtained at the W. M. Keck Observatory, which is operated as a scientific partnership among the California Institute of Technology, the University of California, and the National Aeronautics and Space Administration. The Observatory was made possible by the generous financial support of the W. M. Keck Foundation. Observations at the Palomar Observatory were made as part of a continuing collaboration between the California Institute of Technology and Cornell University. The 60-inch telescope at Palomar Mountain is jointly owned by the California Institute of Technology and the Carnegie Institution of Washington.

[2] Space Sciences Building, Cornell University, Ithaca, NY 14853; jcw14@cornell.edu

[3] Infrared Processing and Analysis Center, M/S 100-22, California Institute of Technology, Pasadena, CA 91125; davy@ipac.caltech.edu

[4] Infrared Processing and Analysis Center, M/S 100-22, California Institute of Technology, Pasadena, CA 91125; gizis@whitesands.ipac.caltech.edu

[5] Department of Astronomy, University of Massachusetts, Amherst, MA 01003; skrutski@north.astro.umass.edu

[6] U.S. Naval Observatory, P.O. Box 1149, Flagstaff, AZ 86002; dgm@nofs.navy.mil

[7] Space Sciences Building, Cornell University, Ithaca, NY 14853; jrh13@cornell.edu

[8] Unless otherwise stated we use the term 'separation', (Δ), to mean 'apparent separation.'

[9] We define $q \equiv m_{sec}/m_{pri}$, and use the term 'low mass ratio' to mean q near zero.

a field L1 V can either be a very old and VLM star or a less massive, young brown dwarf that is slowly cooling to later spectral types. Binary systems can be used to break this degeneracy and provide examples of L-dwarfs with estimated masses as follows: assuming that the primary and low-mass companion in a system are coeval, age estimates from the primary can be adopted for the secondary. The ages along with inferred effective temperatures can then be used to determine crude mass estimates from theoretical evolutionary curves. Metallicity and distance information is also acquired for L-dwarfs in binary systems from known properties of the primaries.

There are six previously discovered L-dwarfs that are wide separation ($\Delta \geq 100$ AU) companions to nearby stars (see Kirkpatrick et al. (2001), Table 7a, for a summary), including three from 2MASS. The latter were L-dwarf candidates found to be serendipitously located close on the sky to known nearby stars. In this paper we present the first results from a *dedicated* 2MASS search for L-dwarf candidates in close proximity on the sky to known nearby stars. The search area around any given candidate primary is an annulus with inner radius defined by the object brightness and the capability of the 2MASS point source extraction algorithm to identify faint objects adjacent to bright sources. The outer radius is defined by the distance to the primary and the maximum companion separation plausible from dynamical binding considerations. The candidate primaries are mainly drawn from the Catalogue of Nearby Stars (Gliese & Jahreiss 1991) and other nearby objects discovered more recently. A future paper will discuss in more detail the search criteria and success rate. In this paper we present two confirmed (spectroscopic and common proper-motion) companions discovered while searching the vicinity of two 'Gliese' objects: 2MASSW J0912145+145940 (L8 V companion to a G8 V+K1 V spectroscopic binary) and 2MASSW J1620261-041631 (L2.5 V companion to an M0 V).

We also present the spectroscopically (but not common proper-motion) confirmed candidate companion 2MASSI J1022148+411426 (L0 V).[10] This object was an L dwarf candidate discovered serendipitously to be nearby on the sky to HD 89744Ab, an F7 IV-V + giant planet system. Motivated by this discovery, we will add all stars with known planets to the list of candidate primaries for the dedicated search.

2MASS survey observations and evidence of common proper motion are discussed in §2. Red-optical (0.65–1.00 μm) and near-infrared (NIR) spectroscopic follow-up observations are presented in §3, along with a grid of known late-M and L-dwarf NIR spectra for classification in $z'JHK$.[11] Age estimates for the candidates are assigned in §4 based upon known physical characteristics of their primaries. We use these age assignments to determine masses for the candidates using theoretical evolutionary curves. A discussion follows in §5.

2. 2MASS OBSERVATIONS

2.1. *Candidate Selection*

The 2MASS Working Database was used to search for color-selected low-mass candidates in close proximity to nearby stars. The color-selection of late-M and L-dwarfs from NIR surveys is now well established (Kirkpatrick et al. (1999); hereafter K99 and Kirkpatrick et al. (2000); hereafter K00). Because of their low effective temperatures, they possess extreme visual-IR colors, e.g. $R-K_s \geq 5.5$. With the exception of the nearest examples, late-M and L-dwarf infrared candidates will have no optical counterparts on visual sky-survey plates. $<J-K_s>$ for these objects reddens monotonically (allowing for cosmic scatter) from ~ 1.1 for M8 V to a maximum of ~ 2.1 for late L-dwarfs using classifications from the red-optical (K99, K00).

The three wide separation companion candidates followed-up in this paper met the color-selection criteria above, were in close proximity on the sky to known nearby stars, and were bright enough ($K_s \lesssim 14$) for NIR spectral follow-up with the Cornell Massachusetts Slit Spectrograph (CorMASS; Wilson et al. (2001a)) on the Palomar 60-inch telescope. The objects' coordinates, photometric magnitudes and $J-K_s$ colors are listed in Table 1. Finding charts are presented in Figure 1.

EDITOR: PLACE TABLE 1 HERE.

EDITOR: PLACE FIGURE 1 HERE.

The companion candidate 2MASSW J0912145+145940 (hereafter 2M0912+14) has $J-K_s = 1.68$ and $K_s = 14.02$. It has an angular separation of 43″ (881 AU) from the binary Gl 337AB (Fin 347, HIP 45170),[12] which has an Hipparcos measured distance of 20.5 ± 0.4 pc (Perryman et al. 1997). At this distance the companion would have $M_{K_s} = 12.47$. Using the absolute magnitude — spectral class relation of K00,

$$M_{K_s} = 10.450 + 0.127(\text{subclass}) + 0.023(\text{subclass})^2 \quad (1)$$

where subclass is -1 for M9 V, -0.5 for M9.5 V, 0 for L0 V, 0.5 for L0.5 V, etc., we infer a candidate companion spectral type of L7 V. K00 found $<J-K_s> = 1.94$ with $\sigma_{<J-K_s>} = 0.37$ for the L7 subclass, so the color of 2M0912+14 is about 1 σ from the mean.

2MASSW J1620261-041631 (hereafter 2M1620-04) has $J-K_s = 1.72$ and $K_s = 13.59$. It has an angular separation of 35.9″ (1090 AU) from the M0 V Gl 618.1 (G 17-11, HIP 80053), which has an Hipparcos measured distance of 30.3 ± 2.4 pc (Perryman et al. 1997). At this distance the companion would have $M_{K_s} = 11.53$. Using

[10] Objects with designations 2MASSI are part of the Second Incremental Point Source Catalog. Those objects with 2MASSW designations are part of the working point source database (Cutri et al. 2000).

[11] $\acute{z}$ is a SDSS photometric band with $\lambda_c = 0.91\mu$m and $\Delta\lambda = 0.12\mu$m. The long wave cut-off is determined by CCD sensitivity (Fukugita et al. 1996).

[12] The Washington Double Star Catalog identifies Gl 337AB as Fin 347Aa, and lists it as the primary in an astrometric multiple system. The other components are BUP 125 (Aa-B), STT 569 (Aa-C), and SLE 478 (Aa-D). Comparisons of POSS-I and POSS-II images show the three other components to be background objects without common proper motion to Gl 337AB. Aa-B and Aa-D appear to be the same object, simply observed at epochs 1907 and 1984, respectively. At epoch 1984 Aa-C was located 80.1″ from Gl 337AB at position angle ($\phi = 118°$) and Aa-D was located 208.8″ away with $\phi = 208.8°$ (Mason et al. 2001).

Equation (1) we infer L4 V. K00 found $<J-K_s> = 1.87$ with $\sigma_{<J-K_s>} = 0.16$ for the L4 subclass, so the color of 2M1620-04 is also about 1 σ from the mean.

2MASSI J1022148+411426 (hereafter 2M1022+41) has $J-K_s = 1.27$ and $K_s = 13.62$. It has an angular separation of 63.1″ (2460 AU or 0.012 pc) from the F7 IV-V star HD 89744 (HR 4067, HIP 50786), which has an Hipparcos measured distance of 39.0 ± 1.1 pc (Perryman et al. 1997). At this distance the companion would have $M_{K_s} = 10.7$. Using Equation (1) we infer L1 V. K00 found $<J-K_s> = 1.43$ with $\sigma_{<J-K_s>} = 0.21$ for the L1 subclass, so the color of 2M1620-04 is within 1 σ of the mean.

2.2. *Companionship*

The proper motions of the primaries Gl 337AB and Gl 618.1 are 0.58″ yr^{-1} and 0.42″ yr^{-1} (Perryman et al. 1997). The 2MASS survey astrometric uncertainty is $\lesssim 0.15''$ (1 σ; Cutri et al. (2000)) so these motions allow confirmation that the candidates are indeed proper motion companions by comparing two epoch 2MASS survey images separated by at least a few months.

The field containing 2M0912+14 was scanned twice with 2MASS, once on 1997 November 18 and again on 2000 April 26. The scans showed the position of 2M0912+14 to move 0.64″ yr^{-1} towards position angle $\theta = 299$ deg relative to other stars in the field. This relative motion compares well with the Gl 337AB Hipparcos absolute proper motion of 0.58″ yr^{-1} with $\theta = 295.1$ deg, thus confirming common proper motion (CPM) companionship. Hereafter we refer to 2M0912+14 as Gl 337C.

The field containing 2M1620-04 was scanned twice with 2MASS, once on 1999 July 29 and again on 2000 May 30. The scans showed the position of 2M1620-04 to move 0.44″ yr^{-1} towards position angle $\theta = 269$ deg relative to other stars in the field. This relative motion compares well with the Gl 618.1 Hipparcos absolute proper motion of 0.42″ yr^{-1} with $\theta = 273.1$ deg, thus confirming CPM companionship. Hereafter we refer to the primary as Gl 618.1A and 2M1620-04 as Gl 618.1B.

The proper motion of HD 89744 is only 0.18″ yr^{-1} (Perryman et al. 1997), so a longer baseline is needed to confirm CPM companionship. This field was scanned once with 2MASS on 1998 April 05. The Palomar Observatory Sky Survey II (POSS-II) also weakly detected 2M1022+41 in the photographic NIR passband (IVN plate + RG9 filter — $\lambda_{eff} \sim 8500$ Å; Reid et al. (1991)) on 1998 December 30. Unfortunately, the nine month baseline between the 2MASS and POSS-II images is not sufficient to establish common proper motion.

We can, however, assess the probability that 2M1022+41 is an unassociated low-mass object based upon the likelihood that an L-dwarf such as this object would be found in the same line of sight as HD 89744. The surface density on the sky of 2MASS L-dwarfs to $K_S = 14.7$ is 1 per 20 square degrees (K99). There are ~ 6900 stars within 50 pc listed in the Hipparcos Catalogue; the SIMBAD database contains ~ 7300. Using the larger of the two estimates, less than one 2MASS L-dwarf will be randomly found within 65″ of *any* of the ~ 7300 cataloged stars. In addition, the correlation between the estimated spectral type of 2M1022+41 from K_S and the distance of the suspected primary, L1 V (§2.1 above), and its actual spectral type of L0 V from red-optical spectroscopy (§3.1.1 below) strongly supports companionship. Based on these arguments we consider it safe to assume companionship and hereafter refer to the primary as HD 89744A and 2M1022+41 as HD 89744B. Korzennik et al. (2000) have discovered a planet circling the F star, and we shall refer to this planet as HD 89744Ab.

3. SPECTROSCOPIC FOLLOW-UP

3.1. *Optical Spectroscopy*

3.1.1. *Observations*

Red-optical spectra of the candidates were obtained with the Low Resolution Imaging Spectrograph (LRIS; Oke et al. (1995)) at the 10 m W. M. Keck Observatory (Keck I). A 400 groove mm^{-1} grating blazed at 8500 Å with a 1″ slit and a Tektronics 2048×2048 CCD were used to yield 1.9 Å pixel^{-1} (9 Å resolution) spectra spanning the wavelength range 6300 – 10100 Å. An OG570 blocking filter was utilized to exclude second order. Further details regarding data acquisition and reduction are given in K99 and K00. Table 2 summarizes observations.

EDITOR: PLACE TABLE 2 HERE.

Figure 2 displays the reduced optical spectra. The spectra have not been corrected for telluric absorption. They confirm that the objects are L-dwarfs. Using the L-dwarf classification scheme of K99 we assign the following spectral types: Gl 337C (L8 V), Gl 618.1B (L2.5 V), and HD 89744B (L0 V). These spectral types correspond to effective temperatures of L8 V ($1300 - 1600$ K), L2.5 V ($1800 - 1950$), and L0 V ($2000 - 2200$), where the lower and upper limits are from the classifications schemes of K00 and Basri et al. (2000), respectively.

EDITOR: PLACE FIGURE 2 HERE.

3.1.2. *Lithium*

The Li I (6708 Å) feature is an important indirect gauge of mass (Rebolo et al. 1992). When seen in absorption in all but the youngest fully convective very low-mass objects, this feature indicates insufficient mass ($M \lesssim 60 M_{jup}$, i.e. sub-stellar) to produce central temperatures high enough ($T_{cen} > 2 \times 10^6 K$) to fully fuse the primordial lithium through (p, α) reactions (see e.g. Nelson et al. (1993)). Lithium is not detected in any of the objects to the following equivalent width (EW) upper limits: < 1 Å for Gl 337C and Gl 618.1B, and < 0.5 Å for HD 89744B. This indicates that Gl 618.1B and HD 89744B have $M \gtrsim 60 M_{jup}$, an important mass constraint on the secondaries that we will utilize in §5.1.

Gl 337C is too cool to use the lithium test. As temperatures fall in the atmospheres of L-dwarfs, lithium is expected to give way to LiCl as the dominant lithium bearing gas for $T_{eff} \lesssim 1500 - 1550 K$, thereby depleting existing atomic lithium (Lodders 1999). Since our assigned T_{eff} upper limit for Gl 337C (1600 K) is only slightly warmer than this transition temperature, we consider the use of this test misleading for this object. K00 found diminishing Li absorption line strengths for L7 and L8 dwarfs

when present, and interpreted this as evidence of increasing lithium bearing molecular formation.

LiCl spectral band heads occur in the mid-infrared at 14.51μm ($\nu = 0-1$), 14.71μm ($\nu = 1-2$), and 14.92μm ($\nu = 2-3$) (Klemperer et al. 1960). Unfortunately, these wavelengths are not accessible from the ground due to atmospheric absorption just beyond the N passband, but they will be observable with the Infrared Spectrograph (IRS) on the upcoming Space Infrared Telescope Facility (SIRTF).

3.1.3. Hα

Hα seen in emission is an important measure of chromospheric activity (and youth) in early-mid M-dwarfs, just as Ca II H and K lines are used for FGK stars. Hα emission is not detected with upper limits < 1 Å for Gl 337C and < 0.5 Å for HD 89744B. Gl 618.1B is a possible detection with $EW_{Li} \leq 1$ Å. These results are compatible with the L-dwarf activity statistics from the K99 and K00 samples, in which Hα emission declined from 60% (80% if marginal detections are included) for L0 V to 8% (25% including two marginal detections) for L8 V (Gizis et al. 2000). Statistically we might have expected emission in HD 89744B, but it is not surprising that Gl 618.1B and Gl 337C are not active.

3.2. *Near-Infrared Spectroscopy*

The wavelength of peak energy emission shifts redward into the NIR with decreasing effective temperature, so L-dwarfs become very faint in the red-optical. As noted in K99, a large aperture telescope is needed to use red-optical spectral typing schemes effectively. Because a more practical means of assigning spectral types to color-selected late-M and L-dwarfs was sought, the Cornell Massachusetts Slit Spectrograph (CorMASS; Wilson et al. (2001a)) was built for use on the Palomar 60-inch telescope. Over 100 new field late-M and L-dwarf candidates have been observed with CorMASS as part of a magnitude-limited spectroscopic survey to improve the statistics of the luminosity function across the stellar—sub-stellar boundary in the solar neighborhood. The instrument has also been used for the spectral confirmation of a bright T-dwarf (Burgasser et al. 2000) and now for the follow-up of some candidate wide separation companions in Gizis et al. (2001b) and this paper.

CorMASS is a prism cross-dispersed low-resolution ($R \sim 300$) near-infrared (NIR) spectrograph. Its 2-dimensional spectral format provides simultaneous coverage from $\lambda \sim 0.75\mu$m to $\lambda \sim 2.5\mu$m (*z'JHK* bands). A 40 lines mm^{-1} grating, blazed at 4.8μm, is used with a fixed 2″ slit to image the raw spectra across 6 orders on a NICMOS 3 detector.

Figure 3 presents a grid of CorMASS NIR spectra for known low-mass objects spanning spectral classes M6–T. An observing log for the grid is presented in Table 3. The M-dwarf spectral types are on the Kirkpatrick, Henry, & McCarthy, Jr. (1991) system, and L-dwarf classifications are on the K99 system. The data reduction technique follows that described in Wilson et al. (2001a). Our grid qualitatively agrees with similar NIR grids of L-dwarfs already published (Reid et al. 2001b; Testi et al. 2001). As seen in Figure 3, the NIR spectra are dominated by molecular absorption features that smoothly change with spectral type through the end of the L-class. The H_2O absorption features bracketing H-band change most obviously. In particular, the slope of the blue side of the H-band spectra appears to increase monotonically with later spectral type as H_2O absorption increases in the L-dwarf atmospheres. This monotonic relationship has been quantitatively confirmed for a grid of L-dwarfs by Reid et al. (2001b) and Testi et al. (2001) and for a grid of M-dwarfs by Jones et al. (1994). Delfosse et al. (1999) also use this feature to help classify DENIS candidate low-mass objects.

EDITOR: PLACE FIGURE 3 HERE.

EDITOR: PLACE TABLE 3 HERE.

Other spectral changes in the grid include varying strengths of the FeH features at 0.99μm and 1.19-1.24 μm, as well as changes in the pair of K I doublets in J-band. The evolution of the J-band features were investigated by McLean et al. (2000) using higher resolution spectra of L-dwarfs. K-band evolution seen in Figure 3 includes increasing H_2O absorption on the blue end, increasing curvature longward of $\sim 2.1\mu$m due to collision induced absorption of H_2, and a deepening of the CO bandhead feature at $\sim 2.3\mu$m (see e.g. Tokunaga & Kobayashi (1999)). The slow spectral evolution for late-M and L-dwarfs is in marked contrast to the rapid change in features observed from L8 V to T dwarfs as the primary carbon-bearing molecule changes from CO to CH_4 .

CorMASS observations of the companions are listed in Table 2. The spectra have been inserted into Figure 3 at positions bracketed by known objects with similar spectra based upon comparisons by eye. The NIR spectra of Gl 337C supports a spectral type assignment of L8 V. The depth of the J-band H_2O ($\sim 1.15\mu$m) absorption feature indicates a spectral type later than L7 V. The spectra of Gl 618.1B (smoothed with a boxcar average of 5 pixels) and HD 89744B are both similar to those of the late-M and early L-dwarfs. Because the spectral features evolve more slowly in this regime we cannot confirm a specific spectral type by eye. The spectra support a range of spectral types: M9 V $>$ SpT$_{Gl618.1B}$ $>$ L3.5 V and M9 V $>$ SpT$_{HD89744B}$ $>$ L2 V.

At the resolution of CorMASS (R $\sim$ 300) quantitative comparison of spectral type indices (i.e. ratios of average flux in specified regions, or equivalent widths, etc.) will be necessary to improve the accuracy of spectral subclass assignments based upon NIR spectra. In a subsequent paper (Wilson et al. 2001b) we will define quantitative spectral indices for assignment of spectral subclass for use with the CorMASS spectroscopic survey of field low-mass object candidates.

4. AGE ESTIMATES

The assignment of ages to field stars is by its very nature imprecise due primarily to few reliable techniques, cosmic scatter, and especially slow evolution for stars with late spectral types. Hopefully the analysis of systems with late-M and L-dwarf wide separation companions will motivate

increased study of 'age dating' techniques. This necessarily lengthy section gathers available evidence and applies relevant techniques to derive unfortunately imprecise age estimates for the primary systems of the L-dwarf companions.

Published age related properties for the three primary systems are summarized in Table 4. A decrease in activity (coronal and chromospheric) with age in stars with convective envelopes is generally attributed to a reduction in the classical dynamo effect (α-Ω) as stars spin down due to angular momentum losses in stellar winds (see e.g. Baliunas & Vaughan (1985))

EDITOR: PLACE TABLE 4 HERE.

Surface lithium abundance from high resolution spectroscopy can serve as a crude age indicator for main sequence stars with convective envelopes. Primordial surface lithium in these stars is destroyed through mixing to warmer interior temperatures due to the combined action of convection in the outer envelope and more complex mechanisms not yet fully understood (Pinsonneault 1997). Only one of the three primaries in this paper have published lithium abundance measurements, namely HD 89744A. Unfortunately, the measurement's usefulness as an age diagnostic is diminished because, as an F7 IV-V, it falls very close to the mid-F 'lithium dip' region of the main sequence in which dramatic surface lithium destruction occurs where standard evolutionary models using convective mixing predict there should be no destruction (see, e.g. Balachandran (1995)).

Space motions are frequently used as indicators of age for samples of stars. But their use in assigning ages to individual stars must be done with great caution due to significant dispersion within any kinematic class. Nonetheless, it is unlikely for an old star to have small velocity, but a young star can have a high velocity. We take the division between *young* and *old* to be $\sim 1.5-2$ Gyr, the division between the young disk and old disk used by Eggen (1989). We will refrain from placing significant weight on kinematic age when possible.

In the case of HD 89744A there are several explicit age determinations already published based upon high resolution metallicity measurements and fits to stellar isochrones. These ages will be compared with our estimates derived from physical properties.

4.1. *Gl 337 System*

Gl 337AB is a double-lined spectroscopic (SB2) and visual binary located 20.5 ± 0.4 pc away (Hipparcos, Perryman et al. (1997)). Astrometric, speckle and visual observations reveal an orbital semi-major axis of $\sim 0.116''$ (~ 2.4 AU) and a period of 2.7 years (see e.g. Pourbaix (2000); Mason et al. (1996)). It is one of the shortest-period visual pairs observed. Published measurements are summarized by Mason et al. (1996). They adopted a spectral type of G8 V for both members based on *ubvy* photometry. More recent lunar occultation (Richichi et al. 2000) and adaptive optics observations (Barnaby et al. 2000) indicated an early K spectral type for the secondary based on ~ 0.1 brighter magnitudes than the primary at K and r bands.

4.1.1. *Age from Coronal Activity*

Gl 337AB is detected as a ROSAT X-ray source with $L_X = 9.3 \times 10^{27}\ erg\ s^{-1}$ (Hünsch et al. 1999). The quantity $R_X = \log L_X/L_{bol}$ is often used to describe X-ray emission in a distance and stellar radius independent logarithmic ratio. Gaidos (1998) has derived a relation between R_X and age for solar type stars using published empirical relations for rotational period time dependence, X-ray luminosity/rotation correlations, and the luminosity evolution of the constant-mass Sun:

$$R_X = -6.38 - 2.64\alpha \log(t/4.6) + \log[1 + 0.4(1 - t/4.6)] \quad (2)$$

The coefficient α, from the rotation period time dependence relation, has published values of 1/2 (Skumanich 1972) and $1/e$ (Walter & Barry 1991). The age t is in Gyr. Following Kirkpatrick et al. (2001) we have adjusted the Equation to give $R_X = -6.38$ (Maggio et al. 1987) for the present solar age of 4.6 Gyr.

Because the individual stars of Gl 337AB are not resolved by ROSAT, and they are close in spectral type, we attribute *ad hoc* half of the observed X-ray luminosity to each star. Using $L_{X,Gl337A} = 4.65 \times 10^{27}\ erg\ s^{-1}$ and $L_{bol,Gl337A} = 0.64 \pm 0.06 L\odot$ (Mason et al. 1996), we calculate $R_X = -5.72$. Equation (2) can then be used to estimate an age of 1.25 Gyr ($\alpha = 1/2$) and 1.7 Gyr ($\alpha = 1/e$) for Gl 337AB.

This estimate implicitly assumes that the total X-ray luminosity measured by ROSAT is merely the sum of individual X-ray emission from *non-interacting* members of a binary system. This assumption is valid. Duquennoy et al. (1992) reviewed physical modes of interaction in binaries with solar-mass primaries. Since both members of Gl 337AB are on the main sequence, interaction modes typical of evolved stars such as stellar wind accretion and Roche-lobe overflow can be rejected. Tidal interactions can circularize and synchronize binary orbits for systems on the order of $P \sim 10$ days, i.e. close binaries, and this interaction is thought to cause the P cut-off below which all close binaries have circular and presumably synchronized orbits (see e.g. DM91 Figure 5). Tidal interaction in close binaries nullifies the use of X-ray emission as an indicator of age since the tidal effects disrupt the spin-down, and thus rotation-activity correlation, of the individual stars.

But timescales for orbital synchronization (t_{sync}) and circularization (t_{circ}) for stars with convective envelopes are extremely steep functions of binary fractional separation (a/R): $t_{sync} \propto (a/R)^6$ and $t_{circ} \propto (a/R)^8$ (Zahn 1977). Zahn (1977) estimated $t_{sync} \sim 10^4((1+q)/2q))^2 P^4$ years, where q is the mass fraction and P is the orbital period in days. Using $q \sim 0.96$ and $P \sim 985$ days for Gl 337AB gives $t_{sync} \sim 10^{16}$ years. Gl 337AB is therefore not a tidally interacting binary.

4.1.2. *Kinematics*

The space motion of Gl 337AB is directed opposite the Galactic center: U = -74 km s^{-1}, V = -2 km s^{-1}, and W = $+3$ km s^{-1} (Eggen 1998). (This is with respect to the sun and with U positive towards the galactic center.) This motion makes it a member of the kinematic old disk population with an age of ~ 2 to 10 or 12 Gyr based upon its position outside of the young disk 'Eggen box' in the

UV plane (Eggen 1989). The 'Eggen box' is roughly defined by -50 km s^{-1} $<$ U $<$ $+20$ km s^{-1} and -30 km s^{-1} $<$ V $<$ 0 km s^{-1}.

4.1.3. *Age from Isochrone Comparisons*

Since the Gl 337AB system is both an SB2 and visual binary, mass and magnitude measurements for both components have been published. If we assume that the stars of the binary are coeval, plotting the observed magnitudes against model evolutionary cooling curves *individually* for the components should indicate the same age.

We assumed the mass estimates of $M_A = 0.89 \pm 0.029 M_\odot$ and $M_B = 0.85 \pm 0.026 M_\odot$ (Pourbaix 2000) and absolute magnitudes of $M_{K_{FIRPO}} = 3.94$ and $M_{K_{FIRPO}} = 4.04$, inferred from lunar occultation measurements (Richichi et al. 2000) and Hipparcos distances, for the components. The measured absolute magnitudes were transformed to the appropriate K passbands for comparison with the theoretical zero-metallicity evolutionary models (M_K vs. age) of Baraffe et al. (1998) and Girardi et al. (2000).

Surprisingly, we found disparate ages of roughly 1 Gyr and 3 Gyr for components A and B, respectively, when compared to both models. The most obvious discrepancy was the factor of 2 difference between the observed ($\Delta M_{K_{CIT}} = 0.10$) and predicted ($\Delta M_{K_{CIT}} \sim 0.2$) differential magnitudes for mass differences of $\sim 0.05 M_\odot$. Assuming larger published mass differentials for the components increases the discrepancy. There are no other published K band measurements.

It should be noted that the masses of the components fall within an area of extreme sensitivity to model mixing parameter, metallicity, and initial He abundance, as well as other model assumptions (I. Baraffe 2001, private communication). These complexities likely contribute to the age disparity, but it is unlikely that they fully account for the discrepancy given in particular the Baraffe et al. (1998) model's success in other empirical–theoretical comparisons (see e.g. Delfosse et al. (2000)). While we cannot use these isochrone comparisons to constrain an age for the Gl 337 system, the discrepancy highlighted by this comparison is worthy of further study both from the standpoint of theoretical modelling and via observation.

4.1.4. *Adopted Age*

We adopt an age span of 0.6 to 3.4 Gyr by simply assuming a factor of 2 uncertainty in the 1.25 – 1.7 Gyr estimate derived from X-ray luminosity. Our adopted age is consistent with the kinematic age if the Gl 337 system is a younger member of the old disk.

4.2. *Gl 618.1 System*

Gl 618.1A is an M0 V star located 30.3 ± 2.4 pc away based on Hipparcos measurements. This particular object has not been extensively studied. It is worth noting that field M-dwarfs are notoriously difficult to age date for various reasons, including: 1) slow evolution on the HR diagram in a Hubble time, 2) fast depletion of photospheric lithium since full convection appears as early as M3 V, 3) generally slow rotation, 4) poorly correlated rotation and activity strength (Reid & Hawley 2000), and 5) intrinsic faintness.

4.2.1. *Activity*

Gl 618.1A does not display evidence of chromospheric or coronal activity: ROSAT did not detect X-ray emission from the vicinity of this object, and Hα was observed in absorption on two occasions separated by a decade (Soderblom 1985; Reid et al. 1995). It would actually be unusual if Gl 618.1A displayed evidence of activity since only 8% of 98 M0 V dwarfs observed by Hawley et al. (1996) were magnetically active (dMe).[13] Hawley et al. (1996) found that in a sample of nearly 600 nearby M-dwarfs, the dMe stars ($\sim$ 20% of the sample) came from a kinematically younger population than the remaining dM stars in the survey.

4.2.2. *Previous Age Analysis*

Leggett (1992) classified over 200 low-mass stars into five populations using kinematic and photometric techniques: young disk, young/old disk, old disk, old disk/halo, and halo. The objects in the sample were first placed into populations based upon kinematics. Gl 618.1A's space motion of U = $+122.3$ km s^{-1}, V = -62.2 km s^{-1}, and W = -12.8 km s^{-1} met the criteria for membership in the old disk/halo based upon its eccentricity of $\sim$ 0.5 in the U-V plane. Leggett (1992) also utilized infrared color-color diagrams to estimate mean metallicity ([m/H]). The kinematic populations occupied separate positions on the diagrams, albeit with scatter. Despite its space motion, Gl 618.1A was found to be a member of the young disk on this diagram and was assigned [m/H] $\sim$ 0. The sample photometric uncertainties gave a class membership uncertainty of $\pm$1. Lastly, Leggett (1992) plotted the objects in color-absolute magnitude diagrams and again found the populations could be predicted based upon location. This diagram also supported Gl 618.1A's membership in the young disk.

4.2.3. *Adopted Age*

We are confronted with conflicting and low confidence age diagnostics for this object: large total space motion (138 km s^{-1}) that is unlikely to belong to a young disk ($t < 1.5$ Gyr), and photometric evidence of youth (Leggett 1992). We refrain from adopting a lower limit, and simply allow the lower limit to be set by our non-detection of lithium in the spectrum of the L-dwarf companion (§3.1.2). This imposes a lower limit of $\sim$ 0.5 Gyr (§5.1). We adopt an upper limit age of 12 Gyr based on the recently determined solar neighborhood age of 11.2 ± 0.75 Gyr (Binney et al. 2000).

4.3. *HD 89744 System*

HD 89744A is an F7 star at 39.0 ± 1.1 pc with $M_V = 2.79 \pm 0.06$ based upon Hipparcos measurements (Perryman et al. 1997). Korzennik et al. (2000) summarized this star's properties when they reported the discovery of a massive planetary companion to HD 89744A. The authors adopted a mass of $M = 1.4 \pm 0.09 M_\odot$ for HD 89744A

[13] A dMe is defined as a star with $EW_{H\alpha} > 1$ Å.

based upon the average of independent results from Allende Prieto & Lambert (1999) ($M = 1.34 \pm 0.09 M_{\odot}$) and Ng & Bertelli (1998) ($M = 1.47 \pm 0.01 M_{\odot}$).

The massive planet HD 89744Ab ($m \sin i = 7.2 M_{jup}$) orbits the primary every 256 days with a highly eccentric orbit (e = 0.7). The rms residual uncertainty to the orbital fit of the massive planet was 20.5 m s^{-1} (Korzennik et al. 2000). This residual exceeded the instrumental uncertainties of 10 m s^{-1} and led the authors to state that they could not rule out the existence of a distant companion. A crude estimate of the velocity of the massive planet HD 89744Ab induced by the wide L-dwarf companion HD 89744B is $v \sim a \times \triangle t_{data} = (\mathrm{G}m/r^2) \times \triangle t_{data}$, where a is the acceleration of the planet due to the gravitational force of the L-dwarf, $\triangle t_{data}$ is the ~ 3 year time span of Korzennik et al. (2000) radial velocity observations, $m \sim 0.08 M_{\odot}$ is the mass of L-dwarf, and $r = 2500$ AU. This gives $v \sim 0.007$ m s^{-1}, thus ruling out the possibility that HD 89744B is the cause of the orbital fit residuals. At 2500 AU separation, a companion must be $m \sim 100 M_{\odot}$ to induce a residual radial velocity equal to the instrumental uncertainty of the Korzennik et al. (2000) observations. Of course this does not rule out the possibility of another as yet unseen companion at a smaller orbital separation.

4.3.1. *Ages from Isochrone Fitting*

The age of HD 89744A has been estimated from fits to evolutionary isochrones on three occasions. Edvardsson et al. (1993) calculated an age of 2.09 Gyr using [Fe/H] = 0.18. The object fell within the 'hook-region' of the isochrones used by Edvardsson et al. (1993), so the authors noted that the age could be underestimated by 0.15 dex, corresponding to an older age of 2.95 Gyr. Ng & Bertelli (1998) also calculated an age with this metallicity but used more recent stellar isochrones and Hipparcos distances. They gave an age of 2.04 Gyr. And Gonzalez et al. (2001) derived an age of 1.8 Gyr from isochrone fits. All three ages are in close agreement.

4.3.2. *Luminosity Class*

Saar & Brandenburg (1999) revised this object's luminosity class from main-sequence to subgiant using the improved M_V and hence more accurate location in color magnitude diagrams afforded by Hipparcos results. This change is supported by the finding of Edvardsson et al. (1993) that HD 89744A was within the 'hook-region'. Bartkevičius & Lazauskaitė (1996) assigned a spectral type of F7 IV-V using the Vilnius Photometric System. Ng & Bertelli (1998), using updated isochrones and Hipparcos distances as well, still found the object to be in luminosity class V. Due to the uncertainty in luminosity class we will refer to the object as an F7 IV-V. Based on the object's proximity to the main sequence turn-off, its age can be estimated to be ~ 2 Gyr, the approximate turn-off age of an $M = 1.4 M_{\odot}$ star with our adopted metallicity ([Fe/H] = 0.24; Table 4) from the Bertelli et al. (1994) isochrones used by Ng & Bertelli (1998).

The projected rotational velocity ($v \sin i$) of 8 km s^{-1} (Hoffleit & Warren 1991) for HD 89744A supports a spectral type of F7 IV-V. This rotation falls squarely in the 0 to 20 km s^{-1} range found in a study of late-F subgiants by Balachandran (1990). More recently De Medeiros et al. (1997) and Lèbre et al. (1999) found a sharp rotational discontinuity at $B-V \sim 0.55$, or F8 IV. The rotational velocities of subgiants earlier than F8 spanned from a few to ~ 180 km s^{-1}, while subgiants later than F8 had mean rotational velocities of 6 km s^{-1} at G0 decreasing to ~ 1 km s^{-1} at K5. Abrupt magnetic braking with the deepening convective envelope in the subgiant phase is thought to be the cause of this discontinuity (Lèbre et al. 1999). While there is significant scatter in the rotational velocities of mid to late F-dwarfs, the $v \sin i$ of HD 89744A is compatible with a subgiant evolving redward towards the F8 IV discontinuity.

4.3.3. *Age from Activity*

Pizzolato et al. (2000) reported an upper limit of $R_X < -5.7$ from ROSAT measurements in their study of X-ray emission from early post-main sequence stars. From Equation (2) this gives a minimum coronal age of 1.2 Gyr ($\alpha = 1/2$) and 1.7 Gyr ($\alpha = 1/e$). But since the X-ray measurement is an upper limit, the age indicated by this method is likely much greater.

Another indicator of activity is $\log(R'_{HK})$, where R'_{HK} is the ratio of chromospheric emission in the Ca II H and K lines and the bolometric luminosity (Noyes et al. 1984). For this indicator chromospheric emission is measured using the Mount Wilson HK pseudo-equivalent width S (see below). We can use a relation between age and R'_{HK} from Donahue (1993) based upon observations of clusters spanning a wide range of ages:

$$\log(t) = 10.725 - 1.334 R_5 + 0.4085 {R_5}^2 - 0.0522 {R_5}^3 \quad (3)$$

where the age t is in years and $R_5 = 10^5 \times R'_{HK}$. Using Equation (3) with $\log(R'_{HK}) = -5.04$ (Soderblom 1985) gives an age of 6.4 Gyr for HD 89744A. Gonzalez et al. (2001) found $\log(R'_{HK}) = -5.12$ and derived an age of 8.4 Gyr using Equation (3) as well.

Chromospheric emission is often measured using the Mount Wilson Ca II index $S \propto [(H+K)/(V+R)]$, where H and K are counts in the Ca II passbands and V and R are counts in violet and red continuum bands adjacent to the H-K regions (Vaughan et al. 1978). Barry (1988) used an empirical relationship between the mean values of $<$S$>$ and $B-V$ to derive an age of 9.9 Gyr.

This gives age estimates from activity ranging from 6.4 to 9.9 Gyr, in marked contrast to the ~ 2 Gyr age from isochrone fits. Why are the chromospheric age estimates above so much older than ages from fits to isochrones? Interestingly, HD 89744A is known to have flat activity cycles (i.e. no evidence of activity cycles such as the 11 year solar cycle). Because of its flat chromospheric emission, Wilson (1968) used this object as a standard in his studies of activity variability. Over a 25 year period the standard deviation of S ($< \sigma_S/S >$) for this object was 1.2% (Baliunas et al. 1995).

Baliunas & Jastrow (1990) postulated that solar-type stars that exhibit prolonged low levels of magnetic activity may be in Maunder Minimum-like phases. If HD 89744A is in such a phase then measures of activity will lead to old age estimates that are misleading. Lastly, we note that evolutionary diagrams predict even $1.25 M_{\odot}$ stars to reach the tip of the red-giant branch in < 5 Gyr (Iben 1967); the $\sim 1.4 M_{\odot}$ HD 89744A would be a white dwarf at the ages predicted by its activity.

4.3.4. *Kinematics*

The space motion of HD 89744A is U = +9.3 km s^{-1}, V = −25.6 km s^{-1}, and W = −13.6 km s^{-1} (Edvardsson et al. 1993). This space motion falls within the UV 'Eggen box' corresponding to the young disk with ages $\lesssim 1.5-2$ Gyr (Eggen 1989).

4.3.5. *Adopted Age*

Based upon the well correlated published ages from isochrone fits, as well as evidence of proximity to the main sequence turn-off, we adopt an age of 1.5-3 Gyr for HD 89744A. We ignore age estimates from activity.

5. DISCUSSION

5.1. *Companion Masses and Colors*

With estimated ages for the L-dwarf companions from §4 and effective temperature estimates from spectral types (§3.1.1), the masses of the L-dwarf companions can be estimated using evolutionary models from Burrows et al. (1997). In Figure 4 error boxes are plotted over the evolutionary curves to represent the range of effective temperatures and ages assigned to the objects. Based on the lithium test results we also use the $60M_{jup}$ curve as the minimum mass boundary for Gl 618.1B since we were unable to constrain a lower limit age from physical properties of this object's primary (§4.2.3). Masses can then be easily determined from the figure: $40M_{jup} \leq M_{Gl337C} \leq 74M_{jup}$, $60M_{jup} \leq M_{Gl618.1B} \leq 79M_{jup}$, and $77M_{jup} \leq M_{HD89744B} \leq 80M_{jup}$. Thus Gl 337C is a brown dwarf, HD 89744B is a very low-mass star, and Gl 618.1B could be either. Properties of the L-dwarf companions are summarized in Table 5.

EDITOR: PLACE FIGURE 4 HERE.

EDITOR: PLACE TABLE 5 HERE.

5.2. *Primary Masses*

The total mass of the SB2 binary Gl 337AB is well constrained from astrometry to be $M_{\odot} = 1.74 \pm 0.15$ (Pourbaix 2000). A mass for Gl 618.1A can be derived using its absolute K magnitude and an appropriate mass-luminosity relation (MLR) for sub-solar mass stars. Using $K_{\rm CIT} = 7.11$ (Leggett 1992) and an Hipparcos distance of 30.3 pc gives $M_K = 4.70$. Henry & McCarthy, Jr. (1993) give an empirically determined MLR of

$$\log M/M_{\odot} = -0.1048(M_K) + 0.3217 \qquad (4)$$

for $M_K = 3.07$ to 5.94. Using Equation (4) we calculate $M_{\rm Gl618.1A} = 0.67M_{\odot}$.

Korzennik et al. (2000) adopted a mass of $1.4 \pm 0.09M_{\odot}$ for HD 89744A from the average of published results. These authors determined $m \sin i = 7.2M_{jup}$ for the extrasolar planet HD 89744Ab. For a large sample Chandrasekhar & Münch (1950) have shown $<\sin i> = \pi/4 = 0.79$. Assuming $\sin i$ for the planet's orbit is reasonably close to this expectation value, the planet's mass will be negligible compared to that of the primary. Hence we adopt a combined mass of $1.4M_{\odot}$ for the primary + planet.

5.3. *System Characteristics*

Based on the primary and secondary masses derived above, upper limit mass ratios for the Gl 337ABC, Gl 618.1AB, and HD 89744AbB systems are 0.04, 0.12, and 0.06, respectively (Table 6). Of the six previously discovered systems with wide-separation L-dwarfs, 4 of 6 have $q < 0.1$. It is interesting to ask how many of these systems meet the sample criteria of the Duquennoy & Mayor (1991) G-dwarf binarity study? Duquennoy & Mayor (1991) (hereafter DM91) specifically take as a sample F7 to G9 stars from the Catalogue of Nearby Stars (second edition; Gliese (1969)) with luminosity class IV-V, V, and VI, declinations above −15°, and trigonometric parallax $> 0.045''$, i.e. stars within 22 pc. Two of the primary systems in their study, Gl 417A and Gl 584AB, have wide-separation L-dwarf companions (Kirkpatrick et al. 2001) that were not found by the DM91 radial velocity studies of the primaries. One of the primaries in this paper, Gl 337AB, meets the DM91 criteria except it was not added to the Catalogue of Nearby Stars (CNS) until the third edition in 1991 (Gliese & Jahreiss 1991) and it was assigned a combined K0 V spectral type. (We adopted the spectral type assignment G8 V + K1 V).

EDITOR: PLACE TABLE 6 HERE.

Given these newly discovered systems and improvements in the already well studied CNS, it would be useful to search for wide binaries around a current DM91 style G-dwarf sample to improve our understanding of the distribution of mass ratios below ~ 0.2.[14]

Returning to the three wide-companions in this paper, we find it interesting to compare these systems to other binaries in $(\log \Delta, q)$ and $(\log \Delta, M_{tot,\odot})$ plots. As discussed in Reid et al. (2001a), it is reasonable that wide binaries will have small q (where $q \equiv m_{sec}/m_{pri}$) since system binding energies are proportional to M_{tot}/q. The three binaries in this paper, all with $q < 0.15$, follow this expectation, as do all previously discovered wide separation binaries with L dwarf companions.

Reid et al. (2001a) also find a characteristic upper limit radius for binary separation as a function of total mass in their $(\log \Delta, M_{tot,\odot})$ plot of L dwarf and M dwarf binaries in the solar neighborhood and HST Hyades and field binaries, where Δ has units of AU. Empirically they find a cut-off defined by the log-normal relation

$$\log \Delta_{max} = 3.33M_{tot,\odot} + 1.1 \qquad (5)$$

The systems Gl 337 and HD 89744 have total masses over $1.5M_{\odot}$ so their separations are at least three orders of magnitude smaller than the maxima predicted by Equation 5. The Gl 618.1B system, an M-dwarf/L-dwarf pair with $M_{tot,\odot} \sim 0.75$ and $\log \Delta = 3.04$, comes closer to the cut-off but is still less than the $\log \Delta_{max} \sim 3.43$ prediction from Equation 5. Thus all three companions have Δ that fall well within the upper limits.

[14] The recent results of extrasolar planet searches will also impact the DM91 results, although then one must address the issue of when does a binary system change its label to primary star + planet. For instance, 51 Peg (Gl 882), with its recently discovered extrasolar planet, is in the DM91 sample.

6. CONCLUSION

We have discovered two wide separation L-dwarf common proper motion companions to nearby stars and identified a third candidate from 2MASS. Spectral types assigned from optical spectroscopy were L0 V, L2.5 V, and L8 V. NIR low resolution spectra of the companions were provided as well as a grid of known objects spanning M6 V – T dwarfs to support spectral type assignment for these and future L-dwarfs in the *z'JHK* bands. Using published measurements, we estimated ages of the companions from physical properties of the primaries. These crude ages allowed us to estimate companion masses using theoretical low-mass star and brown dwarf evolutionary models. We found that Gl 337C is a brown dwarf, HD 89744B is a VLM star, and Gl 618.1B may be either. With the addition of these new L-dwarfs there are nine wide-binary ($\Delta \geq 100$ AU) L-dwarf companions of nearby stars known. These discoveries improve the statistics of binaries involving low-mass stars and brown dwarfs. In particular they support initial conclusions that the 'brown dwarf desert' seen at small separations around main sequence stars does not extend to wide separations. The discovery of these companions in low mass ratio systems ($q \lesssim 0.12$), along with similar discoveries previously reported, will also significantly improve our understanding of the binary mass ratio distribution for $q < 0.2$.

We thank the anonymous referee for helpful comments that led to a more concise manuscript, John Carr for a careful reading of a previous draft, and Adam Burrows for providing his evolutionary curves in electronic format. We thank Andrea Richichi and Isabelle Baraffe for supplying filter curves, and Isabelle Baraffe and France Allard for helpful discussions. We also wish to thank the Palomar Night Assistants Skip Staples and Karl Dunscombe for their expertise and support. This publication makes use of data from the Two Micron All Sky Survey, which is a joint project of the University of Massachusetts and the Infrared Processing and Analysis Center, funded by the National Aeronautics and Space Administration and the National Science Foundation. This research has also made use of the SIMBAD database, operated at CDS, Strasbourg, France. DSS images were obtained from the Canadian Astronomy Data Centre, which is operated by the Herzberg Institute of Astrophysics, National Research Council of Canada.

REFERENCES

Allende Prieto, C. & Lambert, D. L. 1999, A&A, 352, 555
Arribas, S. & Roger, C. M. 1989, A&A, 215, 305
Balachandran, S. 1990, ApJ, 354, 310
Balachandran, S. 1995, ApJ, 446, 203
Baliunas, S. & Vaughan, A. 1985, ARA&A, 23, 379
Baliunas, S. & Jastrow, R. 1990, Nature, 348, 520
Baliunas, S., et al. 1995, ApJ, 438, 269
Baliunas, S., Sokoloff, D., & Soon, W. 1996, ApJ, 457, L99
Baraffe, I., Chabrier, G., Allard, F., & Hauschildt, P. H. 1998, A&A, 337, 403
Barnaby, D., Spillar, E., Christou, J. C., & Drummond, J. D. 2000, AJ, 119, 378
Barry, D. C. 1988, ApJ, 334, 436
Bartkevičius, A. & Lazauskaitė, R. 1996, Baltic Astronomy, 5, 1
Basri, G. et al. 2000, ApJ, 538, 363
Bertelli, G., Bressan, A., Chiosi, C., Fagotto, F., & Nasi, E. 1994, Astronomy & Astrophysics Supplement Series, 106, 275
Binney, J., Dehnen, W., & Bertelli, G. 2000, MNRAS, 318, 658
Burgasser, A. J., Wilson, J. C., Kirkpatrick, J. D., Skrutskie, M. F., Colonno, M. R., Enos, A. T., Smith, J. D., Henderson, C. P., Gizis, J. E., Brown, M. E., & Houck, J. R. 2000, AJ, 120, 1100
Burrows, A., Marley, M., Hubbard, W. B., Lunine, J.I., Guillot, T., Saumon, D., Freedman, R., Sudarsky, D., & Sharp, C. 1997, ApJ, 491, 856
Carney, B. W. 1979, ApJ, 233, 211
Chandrasekhar, S. & Münch, G. 1950, ApJ, 111, 142
Cutri, R. M., et al. 2000, Explanatory Supplement to the 2MASS Second Incremental Data Release, http://www.ipac.caltech.edu/2mass/releases/second/doc/explsup.html
De Medeiros, J. R., do Nascimento, J. D., Jr., & Mayor, M. 1997, A&A, 317, 701
Delfosse, X. et al. 1997, A&A, 327, L25
Delfosse, X., Tinney, C. G., Forveille, T., Epchtein, N., Borsenberger, J., Fouqué, P., Kimeswenger, S. & Tiphène, D. 1999, A&ASS, 135, 41
Delfosse, X., Forveille, T., Ségransan, D., Beuzit, J.-L., Udry, S., Perrier, C., & Mayor, M. 2000, A&A, 364, 217
Donahue, R. A. 1993, PhD thesis, New Mexico State University
Duquennoy, A. & Mayor, M. 1991, A&A, 248, 485, DM91
Duquennoy, A., Mayor, M., & Mermilliod, J.-C. 1992, in Binaries as Tracers of Stellar Formation, ed. M. Duquennoy & M. Mayor (Cambridge: Cambridge Univ. Press), 52
Edvardsson, B., Andersen, J., Gustafsson, B., Lambert, D. L., Nissen, P. E., Tomkin, J. 1993, A&A, 275, 101
Eggen, O. J. 1989b, PASP, 101, 366
Eggen, O. J. 1998, AJ, 115, 2397
Epchtein, N. 1997, in The Impact of Large-Scale Near-IR Sky Surveys, ed. F. Garzon (Dordrecht: Kluwer), 15
Fukugita, M., Ichikawa, T., Gunn, J. E., Doi, M., Shimasaku, K., & Schneider, D. P., 1996, AJ, 111, 1748
Gaidos, E. J. 1998, PASP, 110, 1259
Girardi, L., Bressan, A., Bertelli, G., & Chiosi, C. 2000, Astronomy & Astrophysics Supplementary Series, 141, 371
Gizis, J. E., Monet, D. G., Reid, I. N., Kirkpatrick, J. D., Liebert, J., & Williams, R. J. 2000, AJ, 120, 1085
Gizis, J. E., Kirkpatrick, J. D., Burgasser, A., Reid, I. N., Monet, D. G., Liebert, J. & Wilson, J. C. 2001a, ApJ, 551, 163
Gizis, J. E., Kirkpatrick, J. D., & Wilson, J. C. 2001b, AJ, 121, 2185
Gliese, W. 1969, Catalogue of Nearby Stars (2nd ed.; Heidelberg: Astron. Rechen-Institut)
Gliese, W. & Jahreiss, H. 1991, Preliminary Version of the Third Catalogue of Nearby Stars (Heidelberg: Astron. Rechen-Institut)
Gonzalez, G., Laws, C., Tyagi, S., & Reddy, B. E. 2001, AJ, 121, 432
Hawley, S. L., Gizis, J. E., & Reid, I. N. 1996, AJ, 112, 2799
Henry, T. J. & McCarthy, D. W., Jr. 1993, AJ, 106, 773
Hoffleit, D. & Warren, W. H., Jr. 1991, The Bright Star Catalogue, 5th Revised Ed. (Preliminary Version)
Hünsch, M., Schmitt, J. H. M. M., Sterzik, M. F., & Voges, W. 1999, A&ASS, 135, 319
Iben, I., Jr. 1967, ApJ, 147, 624
Jones, H. R. A., Longmore, A. J., Jameson, R. F., & Mountain, C. M. 1994, MNRAS, 267, 413
Kirkpatrick, J. D., Henry, T. J., & McCarthy, D. W., Jr. 1991, ApJS, 77, 417
Kirkpatrick, J. D., et al. 1999, ApJ, 519, 802, K99
Kirkpatrick, J. D., Reid, I. N., Liebert, J., Gizis, J. E., Burgasser, A. J., Monet, D. G., Dahn, C. C., & Nelson, B. 2000 AJ, 120, 447, K00
Kirkpatrick, J. D., Dahn, C. C., Monet, D. G., Reid, I. N., Gizis, J. E., Liebert, J., & Burgasser, A. J. 2001, AJ, 121, 3235
Klemperer, W., Norris, W. G., & Büchler, A. 1960, J. Chem. Phys., 33, 1534
Korzennik, S. G., Brown, T. M., Fischer, D. A., Nisenson, P., & Noyes, R. W. 2000, ApJ, 533, L147
Lèbre, A., de Laverny, P., de Medeiros, J. R., Charbonnel, C., & da Silva, L. 1999, A&A, 345, 936
Leggett, S. K. 1992, ApJS, 82, 351
Lodders, K. 1999, ApJ, 519, 793
Maggio, A., Sciortino, S., Vaiana, G. S., Major, P., Bookbinder, J., Golub, L., Harnden, F. R., & Rosner, R. 1987, ApJ, 315, 687
Marcy, G. W. & Butler, R. P. 2000, PASP, 112, 137
Mason, B. D., McAllister, H. A., & Hartkopf, W. I. 1996, AJ, 112, 276
Mason, B. D., Wycoff, G. L., & Hartkopf, W. I., The Washington Double Star Catalog, U. S. Naval Observatory, http://ad.usno.navy.mil/proj/WDS/wds.html, updated 2001 Mar 05
McLean, I. S. et al. 2000, ApJ, 533, L45

Nelson, L. A., Rappaport, S., & Chiang, E. 1993, ApJ, 413, 364
Ng, Y. K., & Bertelli, G. 1998, A&A, 329, 943
Noyes, R. W., Hartmann, L. W., Baliunas, S. L., Duncan, D. K., & Vaughan, A. H. 1984, ApJ, 279, 763
Oke, J. B., et al. 1995, PASP, 107, 375
Perryman, M. A. C. et al. 1997, A&A, 323, L49
Pinsonneault, M. 1997, ARA&A, 35, 557
Pizzolato, N., Maggio, A., & Sciortino, S. 2000, A&A, 361, 614
Pourbaix, D. 2000, A&AS, 145, 215
Rebolo, R., Martín, E. L., & Magazzù, A. 1992, ApJ, 389, L83
Reid, I. N. et al. 1991, PASP, 103, 661
Reid, I. N., Hawley, S. L., & Gizis, J. E. 1995, AJ, 110, 1838
Reid, I. N., Kirkpatrick, J. D., Gizis, J. E., Dahn, C. C., Monet, D. G., Williams, R. J., Liebert, J., & Burgasser, A. J. 2000, AJ, 119, 369
Reid, I. N. & Hawley, S. L. 2000, New Light on Dark Stars (Springer-Verlag: Berlin), 196
Reid, I. N., Gizis, J. E., Kirkpatrick, J. D., & Koerner, D. W. 2001a, AJ, 121, 489
Reid, I. N., Burgasser, A. J., Cruz, K. L., Kirkpatrick, J. D., & Gizis, J. E. 2001b, AJ, 121, 1710
Richichi, A., Ragland, S., Calamai, G., Richter, S., & Stecklum, B. 2000, A&A, 361, 594
Saar, S. H. & Brandenburg, A. 1999, ApJ, 524, 295
Skrutskie, M. F., et al. 1997, in The Impact of Large-Scale Near-IR Sky Surveys, ed. F. Garzon (Dordrecht: Kluwer), 25
Skumanich, A. 1972, ApJ, 171, 565
Soderblom, D. R. 1985, AJ, 90, 2103
Testi, L. et al. 2001, ApJ, 552, L147
Tinney, C. G., Mould, J. R., & Reid, I. N. 1993, AJ, 105, 1045
Tokunaga, A. T., & Kobayashi, N. 1999, AJ, 117, 1010
Vaughan, A. H., Preston, G. W., & Wilson, O. C. 1978, PASP, 90, 267
Walter, F. M., & Barry, D. C. 1991, in The Sun in Time, ed. C. P. Sonett, M. S. Giampapa, & M. S. Matthews (Tucson: Univ. Arizona Press), 633
Wilson, J. C., Skrutskie, M. F., Colonno, M. R., Enos, A. T., Smith, J. D., Henderson, C. P., Gizis, J. E., Monet, D., & Houck, J. R. 2001a, PASP, 113, 227
Wilson, J. C., Gizis, J. E., Skrutskie, M. F., Miller, N., J. Davy Kirkpatrick, Monet, D. G., & Houck, J. R. 2001b, in preparation
Wilson, O. C. 1968, ApJ, 153, 221
York, D. G., et al. 2000, AJ, 120, 1579
Zahn, J.-P. 1977, A&A, 57, 383

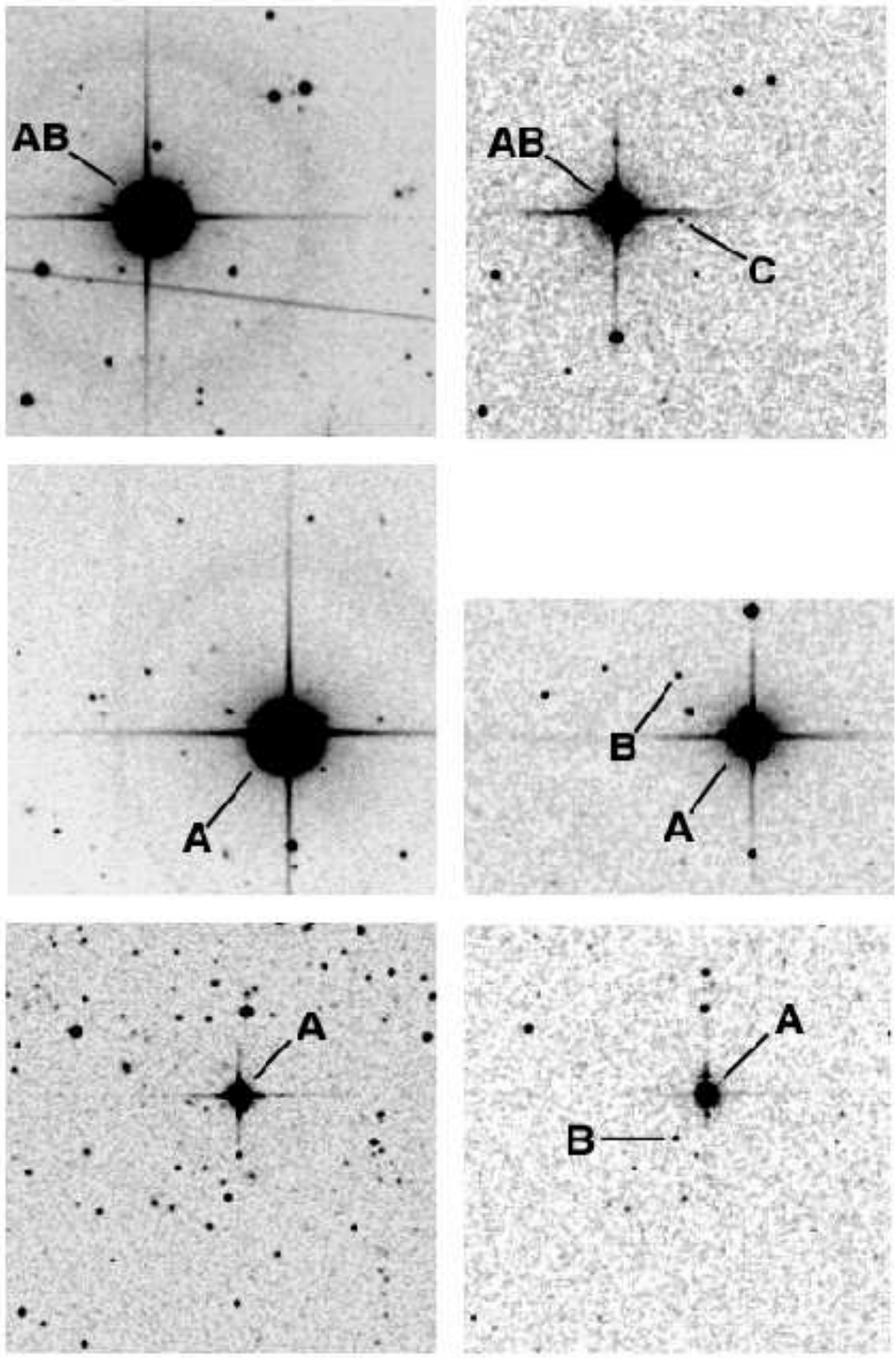

FIG. 1.— Finder charts for all three systems. Images are 5 arcminutes on a side with north up and east to the left. Left panels show DSS red-band images for Gl 337 (epoch 1987.00), HD 89744 (epoch 1990.22), and Gl 618.1 (epoch 1985.44). The primary stars are marked but the new L dwarf companions are invisible here. Right panels show the 2MASS K_s-band images for Gl 337 (epoch 2000.32), HD 89744 (epoch 1998.26), and Gl 618.1 (epoch 2000.41) on which both primary stars and L dwarf companions are labeled. The latent images appearing $\sim 82''$ due south of Gl 337AB and due north of HD 89744A and Gl 618.1A, as well as the triangular-shaped reflection $\sim 11''$ due north of Gl 618.1A, are well characterized bright-star artifacts in 2MASS and should not be confused with real sources.

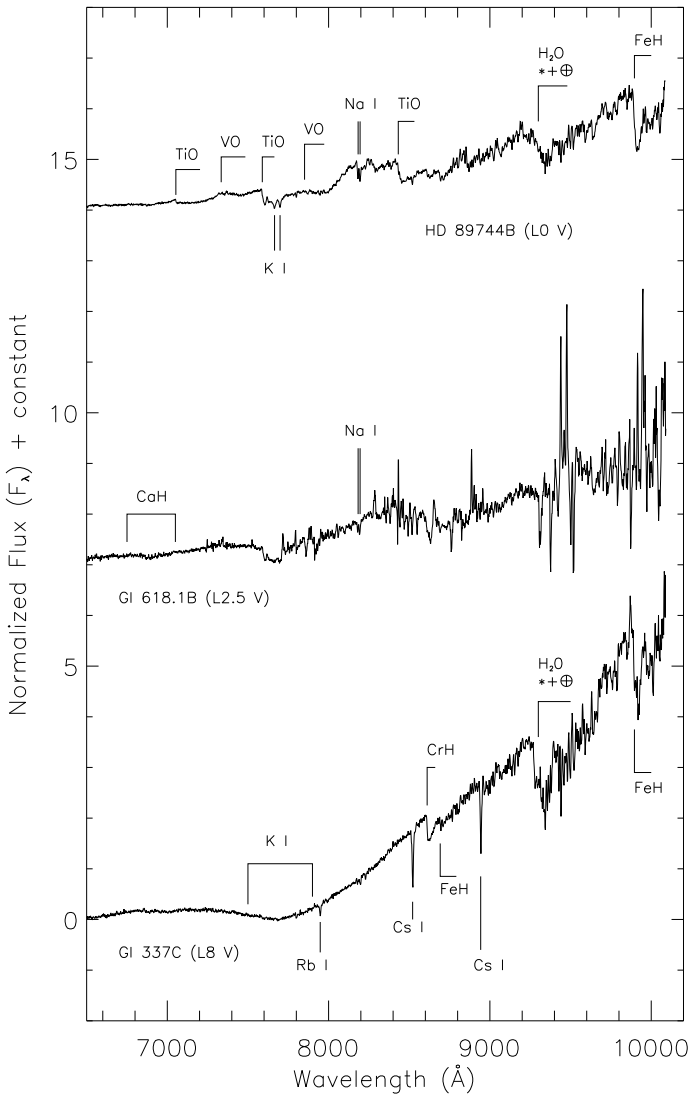

FIG. 2.— Red-optical spectra of the three L-dwarf companions from Keck I. The flux scale is in units of F_λ normalized to one at 8250 Å. Integral offsets have been added to the flux scale to separate the scale vertically. Hallmark features of the L-dwarf class are identified. The Gl 618.1B is very noisy due to observations through cirrus and between episodes of fog.

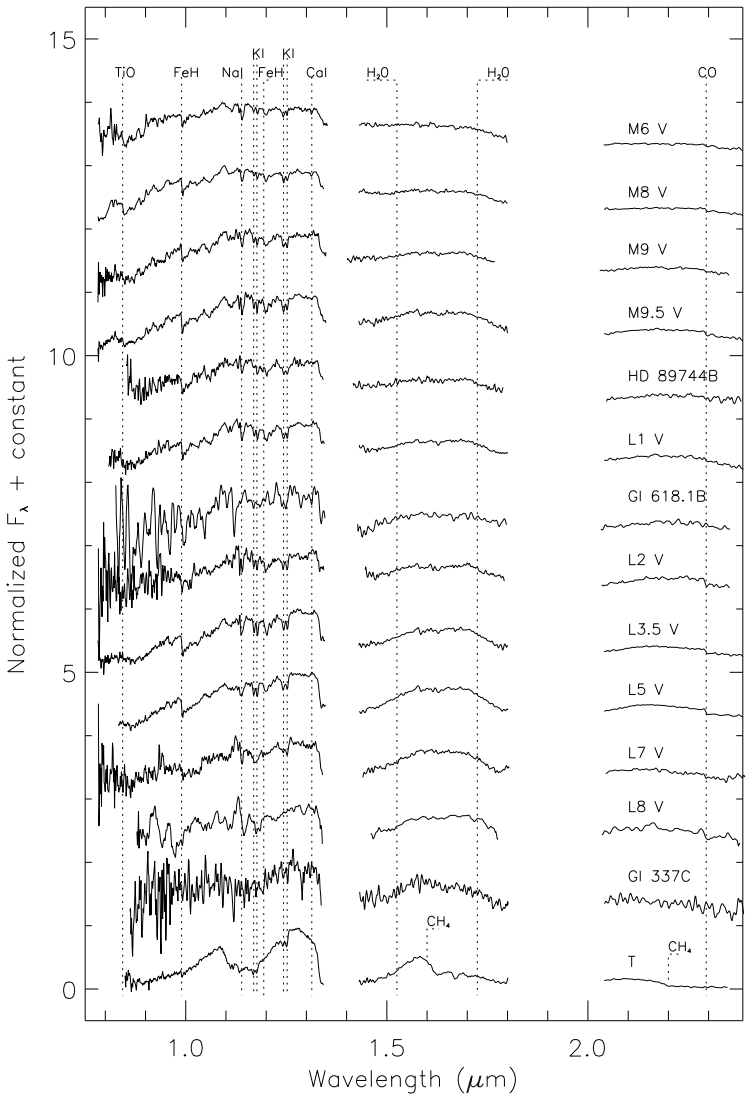

FIG. 3.— A grid of NIR spectra of known low-mass objects with spectral types M6 V – T. Important spectral features are indicated. Data between bands was not usable owing to poor atmospheric subtraction. Spectra have been normalized at the J-band peak and integral flux offsets have been added. The L2 V, L7 V, and L8 V have poor signal-to-noise shortward of $\sim 1.1\mu$m. Spectra of Gl 337C, Gl 618.1B and HD 89744B appear in the grid at positions bracketed by grid objects with similar features. The spectrum of Gl 618.1B has been smoothed with a boxcar average of 5 pixels.

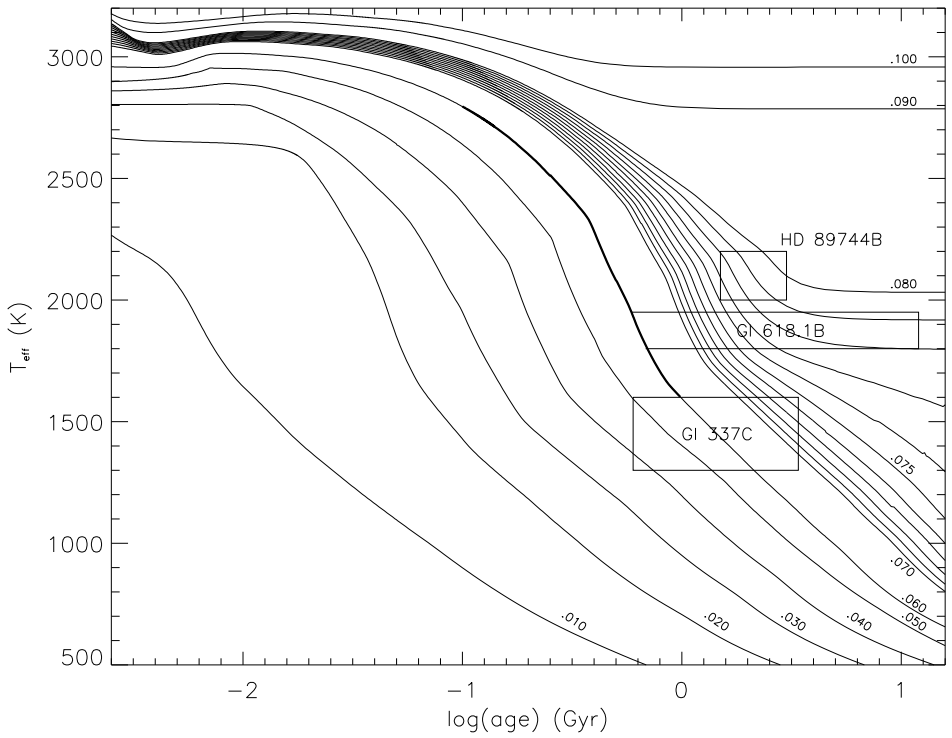

FIG. 4.— Evolutionary models for brown dwarfs and very low-mass stars with masses from $0.010M_{\odot}$ through $0.100M_{\odot}$ from Burrows et al. (1997). The approximate position of the lithium burning cut-off, $0.060M_{\odot}$, is highlighted. Overplotted are error boxes representing the age and T_{eff} estimates we derived for the three companion L-dwarfs.

TABLE 1
CANDIDATE COMPANIONS

Object	RA (2000)	Dec (2000)	J	H	K_s	$J - K_s$
2MASSW J0912145+145940 (2M0912+14)	09:12:14.5	+14:59:40	15.70 ± 0.08	14.59 ± 0.08	14.02 ± 0.06	1.68 ± 0.10
2MASSW J1620261-041631 (2M1620-04)	16:20:26.1	-04:16:31	15.31 ± 0.05	14.32 ± 0.05	13.59 ± 0.04	1.72 ± 0.07
2MASSI J1022148+411426 (2M1022+41)	10:22:14.8	+41:14:26	14.89 ± 0.04	14.04 ± 0.05	13.62 ± 0.05	1.27 ± 0.06

Table 2
Log of Spectroscopic Observations

Object	Obs Date (UT)	Exposure (s)	Telescope	Instrument
2M0912+14 (Gl 337C)	2000 May 10	4000	Palomar 60-inch	CorMASS
···	2000 Dec 26	2400	Keck I	LRIS
2M1620-04 (Gl 618.1B)	2000 May 9	3300	Palomar 60-inch	CorMASS
···	2000 Oct 7	2400	Keck I	LRIS
2M1022+41 (HD 89744B)	2000 May 10	4550	Palomar 60-inch	CorMASS
···	2000 Dec 26	900	Keck I	LRIS

TABLE 3
LATE-M – L-DWARF GRID OBSERVATIONS

Sp T	Object	Obs Date (UT)	Exposure (s)	K_s	K	$J-K_s$	$J-K$	Ref
M6 V	LHS 2034	1999 Oct 27	600	···	10.03	···	0.97	1
M8 V	VB 10	1999 Aug 22	720	···	8.80	···	1.10	1
M9 V	LHS 2924	2000 Jun 16	2400	···	10.67	···	1.17	1
M9.5 V	BRI 0021-0214	1999 Aug 24	1080	···	10.64	···	1.26	2
L1 V	2MASSW J0208183+254253	1999 Aug 24	2700	12.58	···	1.44	···	3
L2 V	2MASSW J0015447+351603	2000 Sep 18	3300	12.24	···	1.58	···	3
L3.5 V	2MASSW J0036159+182110	1999 Aug 24	1440	11.03	···	1.41	···	4
L5 V	2MASSW J1507476-162738	2000 Apr 20	2800	11.30	···	1.52	···	4
L7 V	DENIS-P J0205.4-1159AB	2000 Sep 16	5100	12.99	···	1.56	···	5
L8 V	2MASSW J1632291+190441	2000 Jun 14	5500	13.98	···	1.88	···	6
T	2MASSW J0559191-140448	1999 Oct 24	2400	13.61	···	0.22	···	7

References. — (1) Leggett 1992; (2) Tinney et al. 1993; (3) Kirkpatrick et al. 2000; (4) Reid et al. 2000; (5) Delfosse et al. 1997; (6) Kirkpatrick et al. 1999; (7) Burgasser et al. 2000.

TABLE 4
COMPILED DATA ON WIDE-BINARY PRIMARIES

	Gl 337AB		Gl 618.1A		HD 89744A	
	data	ref	data	ref	data	ref
Spectral Type	G8 V + K1 V[a]	1	M0 V	8	F7 IV-V	11
$B-V$	0.73	2	1.4	9	0.54	10
Distance (pc)	20.5 ± 0.4	3	30.3 ± 2.4	3	39.0 ± 1.1	3
$M_{tot,\odot}$	1.74 ± 0.15	4	0.67[b]	-	1.41[b]	-
Activity						
$\log(L_X/L_{bol})$	-5.69	5,6	not detected	6	< -5.7	12
$\log(R'_{HK})$	...		...		$-5.04,-5.12$	10,13
$H\alpha$ (EW)	...		-0.62 ± 0.35	10	...	
P_{rot} (days)	...		...		9	13
period	...		...		flat	14
Metallicity						
[Fe/H]	-0.14[c]	2,7	...		$+0.24$[d]	15,16
[M/H]	...		~ 0	9	...	
Lithium Abundance						
$\log N_{Li}$	...		...		2.07[e]	16
Kinematics						
U(km/s)[f]	-74	7	$+122.3$	9	$+9.3$	15
V(km/s)	-2	7	-62.2	9	-25.6	15
W(km/s)	$+3$	7	-12.8	9	-13.6	15

[a]Combined spectral type from K0 V to G8 V have been published for this object, with the latter favored by Mason et al. (1996). More recent measurements indicate G8 V + K1 V based upon magnitude differences of the components (Barnaby et al. 2000).

[b]See text §5.1 for derivation.

[c]The average of P[Fe/H] = −0.33, derived from Strömgren photometry (Eggen 1998) and P[Fe/H] = 0.04, derived by Arribas & Roger (1989) using the (U − B) index of Carney (1979).

[d]The average of [Fe/H] = 0.18 (Edvardsson et al. 1993) and [Fe/H] = 0.30 (Gonzalez et al. 2001). Both measurements are from high resolution spectroscopy.

[e]On the scale of $[\log \epsilon(Li_\odot) \equiv \log(N_{Li}/N_H)_\odot + 12 = 1.06]$.

[f]U defined positive towards the Galactic Center (GC). Eggen (1998), Leggett (1992), and Edvardsson et al. (1993) define U positive away from the GC, so their measurements have been multiplied by −1.

References. — (1) Barnaby et al. 2000; (2) Arribas & Roger 1989; (3) Perryman et al. 1997; (4) Pourbaix 2000; (5) Mason, McAlister, & Hartkopf 1996; (6) Hünsch et al. 1999; (7) Eggen 1998; (8) Reid, Hawley, & Gizis 1995; (9) Leggett 1992; (10) Soderblom 1985; (11) Saar & Brandenburg 1999; (12) Pizzolato, Maggio, & Sciortino 2000; (13) Baliunas, Sokoloff, & Soon 1996; (14) Baliunas et al. 1995; (15) Edvardsson et al. 1993; (16) Gonzalez et al. 2001.

TABLE 5
DERIVED SECONDARY PARAMETERS

	Gl 337C	Gl 618.1B	HD 89744B
Spectral Type	L8 V	L2.5 V	L0 V
T_{eff} (K)	$1300 - 1600$	$1800 - 1950$	$2000 - 2200$
Age (Gyr)	$0.6 - 3.4$	$0.5 - 12$	$1.5 - 3.0$
M_{jup}	$40 - 74$	$60 - 79$	$77 - 80$

Table 6
Wide-Binary System Parameters

	Gl 337	Gl 618.1	HD 89744
$M_{tot,\odot}$	$1.77 - 1.81$	$0.73 - 0.75$	1.48
q	$\lesssim 0.04$	$\lesssim 0.12$	$\lesssim 0.06$
Δ (AU)	881	1090	2460